International Journal of Power Electronics and Drive System (IJPEDS)
Vol. 17, No. 1, March 2026, pp. 82~94
ISSN: 2088-8694, DOI: 10.11591/ijpeds.v17.i1.pp82-94

An innovative winding configuration to enhance 3-phase induction motor performance

Zuriman Anthony[1,2], Refdinal Nazir[2], Muhammad Imran Hamid[2]
[1]Department of Electrical Engineering, Faculty of Engineering, Institut Teknologi Padang, Padang, Indonesia
[2]Department of Electrical Engineering, Faculty of Engineering, Universitas Andalas, Padang, Indonesia

Article Info

Article history:

Received May 26, 2025
Revised Oct 20, 2025
Accepted Dec 11, 2025

Keywords:

2-layer design
3-phase induction motor
Coil configuration
Enhance performance
Three-phase power supply

ABSTRACT

A three-phase induction motor is extensively employed in the industrial sector due to its robustness and cost-effectiveness. An enhancement of this motor is underway to optimize its performance. Enhancing motor performance is intricately linked to escalating motor production expenses. Consequently, an innovative strategy is essential to enhance motor performance without incurring substantial extra expenses. This study aimed to introduce a novel approach for designing 3-phase induction motor coils to enhance motor performance without significant additional expenses. This study concentrated on the design of a 3-phase induction motor coil, rated at 1 HP, 380 V, 2 A, 4 poles, and 24 slots, and arranged in a Y-connection. We fabricated the coil using a dual-layer approach, creating magnetic pole pairs on each layer. The study's results demonstrated an improvement in output power, efficiency, load torque, and rotor speed of the new motor design, specifically by 19.32%, 16.26%, 18.48%, and 0.72%, respectively. Despite a 3.05% rise in motor coil current during peak load conditions, the motor's overall performance significantly improves, enhancing its capabilities without considerable additional expenses. This study claims that the suggested way can make other 3-phase induction motors work better without costing a lot more.

Corresponding Author:

Refdinal Nazir
Department of Electrical Engineering, Faculty of Engineering, Universitas Andalas
Limau Manis, Pauh, Padang - 25175, West Sumatra, Indonesia
Email: refdinalnazir@eng.unand.ac.id

1. INTRODUCTION

A 3-phase induction motor is characterized by its straightforward design, durable build, cost-effectiveness, dependability, and straightforward maintenance [1]-[8]. As a result of these advantages, industrial facilities continue to rely heavily on this motor [1]-[12]. The performance of 3-phase induction motors is inferior to that of synchronous motors, although they offer many benefits [1], [2], [13]-[15]. Efforts are currently being made to improve the performance of three-phase induction motors, and multiple approaches are being targeted for improvement [16].

Operating the motor on a single-phase power source is one way to improve the performance of 3-phase induction motors [17], [18]. This can increase the starting torque, power factor, and motor efficiency. When you use a single-phase power source with a three-phase induction motor, you have to pay more for control and capacitor circuits, which are directly related to the motor's power rating [17], [18].

Another effort to make 3-phase induction motors work better is to improve the ferromagnetic materials used in them [19], [20]. Development of ferromagnetic motor materials entails significant additional expenses, as the quality of the material directly correlates with its price escalation [19], [20]. As

the quality of the ferromagnetic material utilized in the motor improves, motor performance enhances; nevertheless, the process also results in elevated production costs due to the increased price of the ferromagnetic material.

Incorporating permanent magnets into the rotor is another way to improve the performance of a 3-phase induction motor [5], [6], [21]. This way can make an induction motor more powerful, have more torque, and work more efficiently. However, the problem arises from the additional costs associated with procuring the permanent magnets used on the rotor [5], [6], [21]. The use of superior permanent magnets in motors leads to elevated production expenses.

Designing the motor coil with more than three phases and making a power source that matches the number of phases in the coil is one way to improve the performance of a three-phase induction motor [22]-[44]. This technique can improve the flux density [38], [39], power [38], [39], torque [34], [35], and efficiency [40], [41] of the motor. In spite of this, adding more phases to the motor coil costs more because a new power source [22]-[37] needs to be developed along with a reliable control system and safety features [23], [27], [29], [30], [40]-[44] that are related to the number of phases and the motor's power output. Because of this, a new way needs to be found to make 3-phase induction motors work better without spending a lot of extra money.

Recent studies demonstrate that optimizing the rotor slot design [45] and motor coil design [38]-[40], [46]-[51] are the most economical approaches to augmenting motor performance. That's why this study suggests making a new type of stator coil for three-phase induction motors so that they work better. As part of this job, a 3-phase induction motor coil with a 2-layer design and different pole configurations for each layer had to be built. We improved the links between the coils to increase the magnetic flux, which improved the motor's work. We tested motors in the lab, looking at how current, speed, total power, and motor efficiency changed when the load changed. The performance of the new motor was compared to that of a standard 3-phase induction motor that had the same stator, rotor, number of stator slots, and number of turns per slot as the new motor. The only difference between the two motors was how the stator coil was set up. Because of this, the newly created 3-phase induction motor did not cost anything extra. The proposed winding design is verified to be suitable for different 3-phase induction motors, improving performance without substantial extra costs.

2. THE COMPREHENSIVE THEORETICAL BASIS

When making a 3-phase induction motor coil, you have to look at several factors, such as the pole pitch, the number of slots, and the number of turns per pole. The following equation can be used to figure out the pole pitch (τ), the number of slots per pole (Q_1), and the number of slots per pole per phase (q_1) coil [52].

$$\tau = {\pi D}/{2p} \quad (1)$$

$$Q_1 = {s_1}/{2p} \quad (2)$$

$$q_1 = {s_1}/{2p\, m_1} \quad (3)$$

In this context, 'D' denotes the stator inner diameter (m), 'π' is defined as 3.14, 'p' represents the number of pole pairs, 's_1' indicates the number of stator slots, and 'm_1' refers to the number of stator coil phases utilized in the induction motor. To define the pole pitch (τ) in relation to the number of slots, use the (4) [52].

$$\tau = {s_1}/{2p} = Q_1 \quad (4)$$

The coil pitch (y) is defined as the distance between two neighboring coil sides in the construction of a single pole [4]. The coil pitch is typically rendered nearly equivalent to the pole pitch. For some applications, the coil pitch may be reduced (corded coils). The coil pitch (y) is determined by counting the slots from the left to the right side of the coil, exactly [52]:

$$y \leq Q_1 \quad (5)$$

The following equation calculates the magnitude of the electrical angle (α_{el}) between two adjacent slots [52].

$$\alpha_{el} = {p\ 360^o}/{s_1} \quad (6)$$

The coil may divide into parallel current channels if the current or voltage in each phase is overly elevated. In a single-layer coil, the maximum number of parallel routes (a) per phase is equal to the number of pole pairs (p); in contrast, in a double-layer coil, this number is twice. A schematic representation of the winding design for a three-phase induction motor is shown in Figure 1. The motor has a double-layer stator with the parameters m1 = 3, $2p$ = 2, and s_1 = 24 at the time [52]. In the winding illustrated in this figure, Q_1 is calculated as 24 divided by 2, yielding 12. This denotes the coil pitch (y) of a full-pitch coil. The coil pitch in this design has been diminished via chording, y = 8 [52].

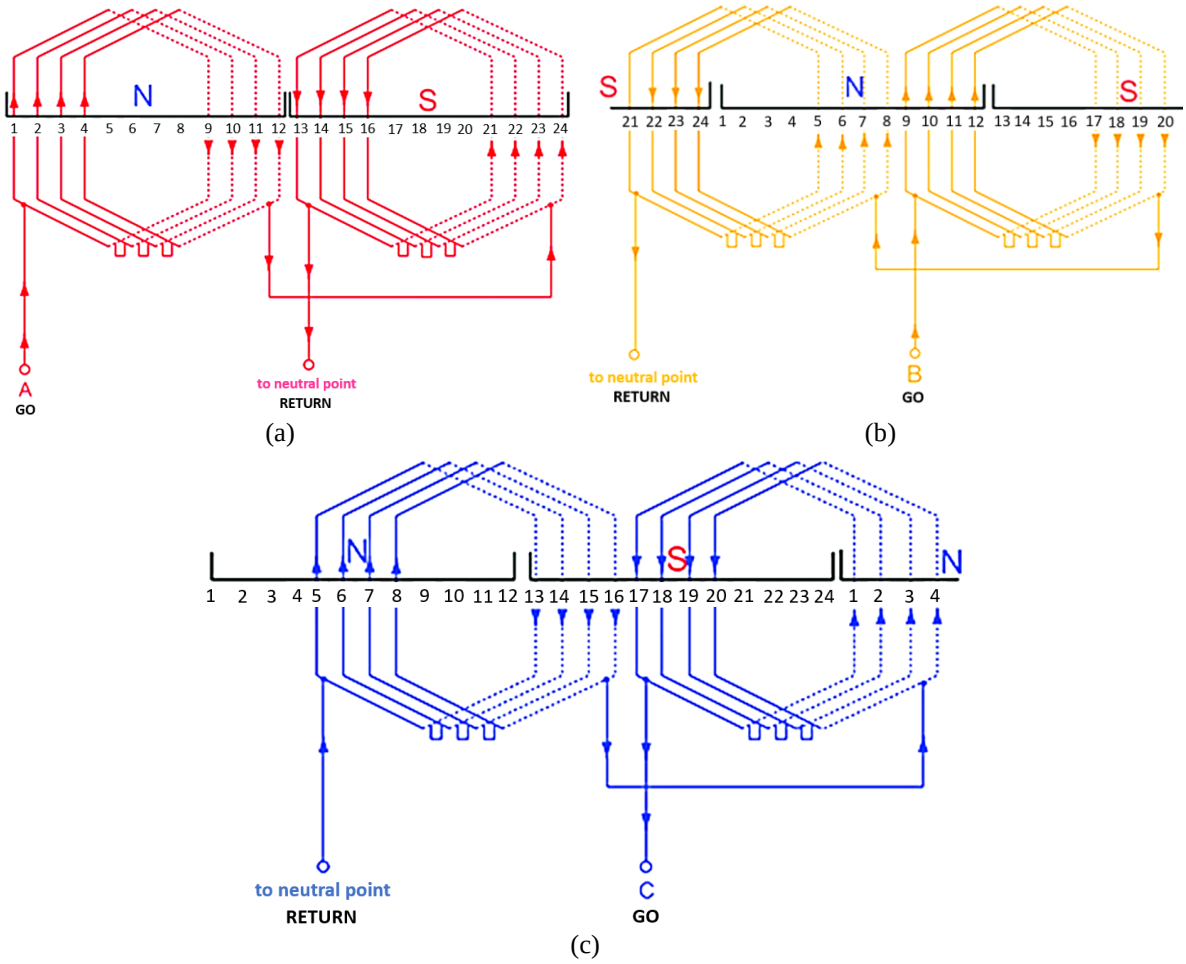

Figure 1. A two-layer configuration in a three-phase induction motor with m_1= 3, 2p = 2, s_1 = 24, y = 8, a = 1, and q_1 = 4: (a) phase A, (b) phase B, and (c) phase C [52]

The motor's ability to move its load is based on the strength of the electrodynamic force (F) it produces when the coil's magnetic field turns. This results in a mechanical torque (T_m) capable of turning the rotor. The link between electrodynamic force (F) and mechanical torque (T_m) is indicated in (7) and (8) [53].

$$F = B.\ i_r.l = (\emptyset\ /A).i_r.l \tag{7}$$

$$T_m = F.r \tag{8}$$

Where '$\emptyset$' means magnetic flux (Wb), 'i_r' is electric current in the rotor conductor (A), 'B' represents magnetic flux density (T), 'l' is the effective length of the rotor conductor (m), 'A' is the cross-sectional area of the rotor (m^2), and 'r' is the rotor radius (m). The average magnetic flux ($\emptyset$) in 1 coil and the magnitude of the stator winding rms EMF (E_1) generated in the stator coil can be calculated as (9) and (10) [52].

$$\emptyset\ = \tau\ L\ B_m\ 2/\pi \tag{9}$$

$$E_1 = \pi\sqrt{2}\, N_1\, k_{w1}\, f\, \emptyset \quad (10)$$

Where L is stator stack length (m), B_m is maximum flux density in the air gap, N_1 is the number of stator coil turns, k_{w1} = winding factor, and f is source frequency. The rotor current referred to as the stator winding (I_2) and the mechanical power converted to drive the rotor (P_m), can then be calculated using (11) and (12) [53].

$$I_2 = {E_1}\Big/{\left(\frac{R_2}{s} + jX_2\right)} \quad (11)$$

$$P_m = 3\,(I_2)^2\,\frac{R_2}{s}\,(1-s) \quad (12)$$

Where s is slip, R_2 denotes the rotor winding resistance as referenced to the stator system (**Ω**), whereas X_2 signifies the rotor winding leakage reactance also referenced to the stator system (**Ω**).

We can calculate the size of the mechanical torque from the coil (T_m), the output power (P_{out}), the load torque (T_L), the input power (P_{in}), and the rotor speed (ω_r), and the efficiency (η) of a 3-phase induction motor using this (13)-(18) [53]:

$$T_m = {P_m}\Big/{\omega_r} \quad (13)$$

$$P_{out} = P_m - P_{rot} \quad (14)$$

$$T_L = {P_{out}}\Big/{\omega_r} \quad (15)$$

$$P_{in} = \sqrt{3}\,.V_{LL}.I_L.Cos\,\varphi \quad (16)$$

$$\omega_r = 2.\pi.Nr/60 \quad (17)$$

$$\eta = (P_{out}\,/P_{in}) \times 100\% \quad (18)$$

where N_r denotes rotor speed (rev/min), V_{LL} represents the line-to-line voltage, I_L signifies line current, and $Cos\,\varphi$ indicates the motor's power factor.

3. METHOD

In the Electrical Engineering Laboratory of the Padang Institute of Technology, the study compared the performance of a brand-new three-phase induction motor to that of a normal three-phase induction motor. Both motors have the same setup regarding their rotor, stator, pole count, stator slot number, coil type, and coil current characteristics. This study is mostly about designing the stator coil for a 3-phase induction motor that needs to work at 50 Hz, 380 V, Y connection, 2 A, 1390 rpm, 24 slots, and 4 poles, and use a 0.6 mm coil with 110 spins per slot. The standard 3-phase induction motor coil is made up of a single-layer coil with 110 turns in each slot. There are two layers of coils in the new design of the three-phase induction motor coil. Each layer has a different 3-phase coil design that is specific to its pole. In the changed motor, each layer has 55 turns, giving each slot a total of 110 turns. We assess how well both motors work by looking at how coil current, speed, torque, and motor efficiency change when different loads are applied. Figure 2 shows how the stator coil of a normal three-phase induction motor is set up. It has 24 slots and 4 poles. There are three coils in this configuration: A, B, and C. In a Y-connection method, the 3-phase supply is connected to terminals A1, B1, and C1, and terminals A2, B2, and C2 are linked together (neutral point). This layout makes the motor work properly.

The new three-phase induction motor includes a stator coil layout with two layers. The first layer mirrors the design depicted in Figure 2, comprising coils A, B, and C, while the second layer, illustrated in Figure 3, consists of coils D, E, and F, achieved by displacing the coil placement by one slot. Figure 2 (first layer) shows that the beginning of the first coil (A1) starts at slot number 1 while Figure 3 (second layer) shows the beginning of the first coil (D1) starts at slot number 2 (shifted 1 slot). Referring to (3) with the number of stator slots 24, 4 pole design, then the distance between 1 slot is 30°, so the coil design is similar to the 30° asymmetrical 6-phase coil design. This new coil design still uses a 0.60 mm coil, but with the number of turns per slot for each layer as many as 55 turns (half of the conventional design), so that the total 1 slot is still filled with 110 turns (the same as the conventional design), so there is no additional cost on the new motor design. The novelty of this research lies in the form of a two-layer coil design created where in this new design a pair of poles (north and south poles) is created on each layer, while in the conventional 2-

layer design the first layer and the second layer are combined to create a common pole pair. Figure 4 illustrates the fundamental difference between the conventional 3-phase induction motor coil design and the proposed new coil design, with Figure 4(a) for a single-layer conventional coil design, Figure 4(b) for a two-layer conventional coil design, and Figure 4(c) for a two-layer proposed coil design, where 'τ' represents the pole pitch of the coil. Figure 4 illustrates that the red line represents the coil in the first layer, while the green line represents the coil in the second layer. To connect the coils of the new motor design as shown in Figure 4(c) using a Y-connection system, the first layer coil connection (Figure 2) must be joined to the second layer coil connection (Figure 3) as shown in Figure 5. In Figure 5, we can see that the 3-phase power sources (L1, L2, and L3) are connected sequentially to the ends of the coils A1, B1, and C1. By using this method, the motor will work like an asymmetrical 6-phase induction motor with better flux density.

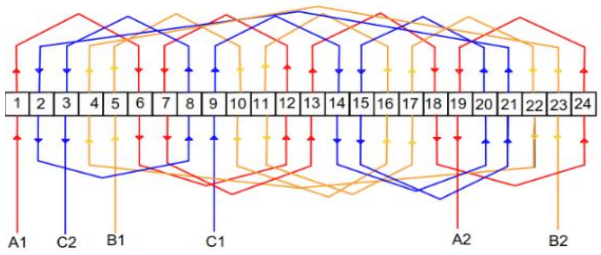

Figure 2. The stator coil design in a standard 3-phase induction motor comprises a 4-pole, 24-slot arrangement

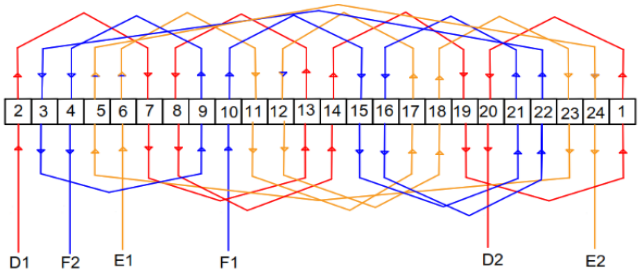

Figure 3. The configuration of the stator coil in the second layer of the novel design for a three-phase induction motor features a four-pole, 24-slot arrangement

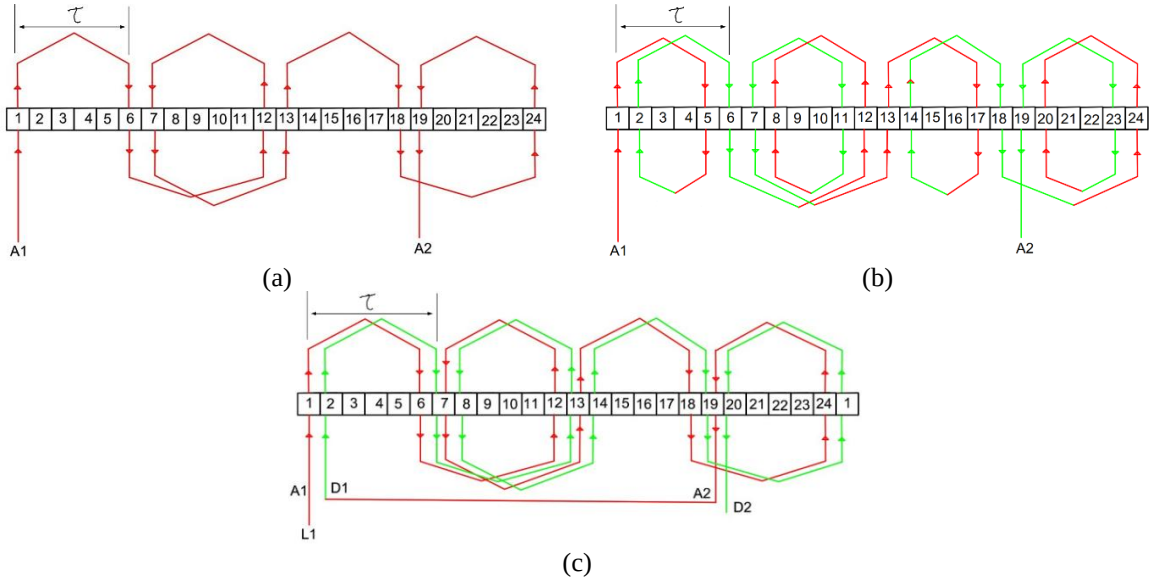

Figure 4. The different forms of 4-pole, 24-slot coil designs for phase A (phase L1) include (a) a single-layer coil conventional design, (b) a two-layer coil conventional design, and (c) a two-layer coil proposed design

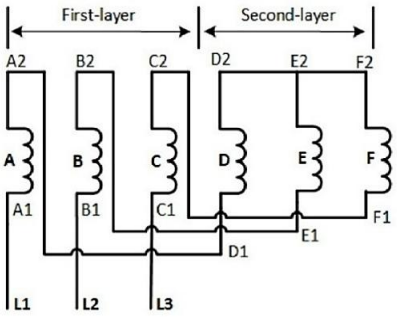

Figure 5. The connection form of the first and the second layer coils of the new design three-phase induction motor

Figure 6 depicts the structure of the induction motor performance testing protocol conducted in the laboratory. Figure 6 depicts the direct coupling of a 3-phase induction motor with a 1-phase induction generator, which is under a gradually increasing incandescent bulb load. A 3-phase electric power source energized the 3-phase induction motor, which then ran the induction generator. The 3-phase induction motor is subjected to various tests by modifying the load provided to it while simultaneously regulating the load of the directly connected induction generator. A 3-phase digital power meter was linked to the motor to measure frequency, current, power factor, voltage, and input power, while a 1-phase digital power meter on the induction generator documented the output in terms of frequency, current, power factor, voltage, and input power. The generator's input power serves as the output power for the 3-phase induction motor, as the motor is directly linked to the generator. The rotor speed is quantified using a digital tachometer, after which load torque and motor efficiency are computed employing (15) to (18). We then displayed the experimental results of the motors' performance in a table and graph for analytical evaluation. To strengthen the analysis of motor characteristics produced by the new coil design in terms of increasing motor output power, motor coil design modeling was also carried out using the 'Ansys Motor-CAD v2024.1.1' program.

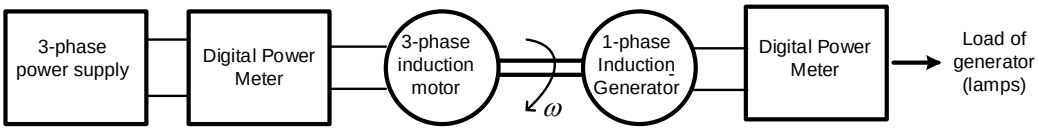

Figure 6. An induction motor performance testing procedure

4. RESULTS AND DISCUSSION

In the lab, we tested how well both traditional and new 3-phase induction motors worked by changing the load on each motor and checking changes in current, speed, load torque, and efficiency. The laboratory testing of both motors yielded performance data illustrated in Figures 7 to 9. Table 1 encapsulates the detailed data on both motor performances. Figures 7 to 9 show that TL (ND), Nr (ND), Pout (ND), Eff (ND), and I (ND) represent the load torque, rotor speed, output power (motor load), efficiency, and coil current in the new design motor. TL(M3), Nr(M3), Pout(M3), Eff(M3), and I(M3) represent the same measurements in the traditional induction motor. Figure 10 shows the design form of the traditional induction motor coil and the new design motor using the 'Ansys Motor-CAD v2024.1.1' program, while Figures 11 and 12 display the simulation results.

It is clear from looking at Figure 7 that the new design 3-phase induction motor has better load power (TL) and rotor speed (Nr) than the old 3-phase induction motor. Looking at Figure 7 and Table 1 shows that the updated design of the 3-phase induction motor can handle a load torque of 5.77 Nm at a speed of 1390 rpm. The normal three-phase induction motor has a peak load torque of 4.87 Nm and a speed of 1380 rpm. The research shows that the new design of the 3-phase induction motor is better than the old one. The load torque (TL) goes up by 18.18%, and the rotor speed goes up by 0.72%. The phenomenon can be explained by the new design of the motor coils, which effectively enhances the pole pitch (τ), as demonstrated in Figure 4(c). The design leads to a rise in the magnetic flux (∅) within the motor, as shown in (9), which in turn causes an increase in 'E_1' and 'P_m', as evidenced in (10) and (12). The increase in 'P_m' results in a proportional increase in 'P_{out}' and 'T_L', as illustrated in (14) and (15). This approach leads to an

observable increase in load torque (T_L) and motor speed (Nr), as demonstrated in Figures 7(a) and 7(b). The increase in flux (∅) in the motor also causes an increase in the flux density (B), which automatically increases the electrodynamic force (F) and mechanical torque (T_m) of the motor as shown in (7) and (8). The results of FEA simulations conducted with 'Ansys Motor-CAD' substantiate this conclusion, as illustrated in Figure 11. From Figure 11, it can be seen that the stator of the newly designed 3-phase induction motor has more brown color, which means it has a higher maximum flux density than the stator of the traditional 3-phase induction motor. Figure 11(a) shows that the conventional 3-phase induction motor only has an air gap flux density of 0.393 Tesla, which is lower than the air gap flux density of the newly designed 3-phase induction motor of 0.4114 Tesla, as shown in Figure 11(b).

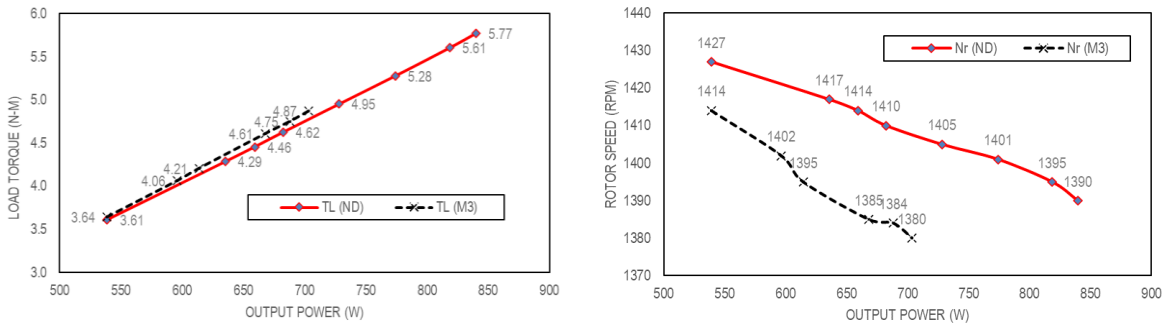

(a) (b)

Figure 7. Characteristics of the correlation between (a) load torque and motor output power and (b) rotor speed and motor output power

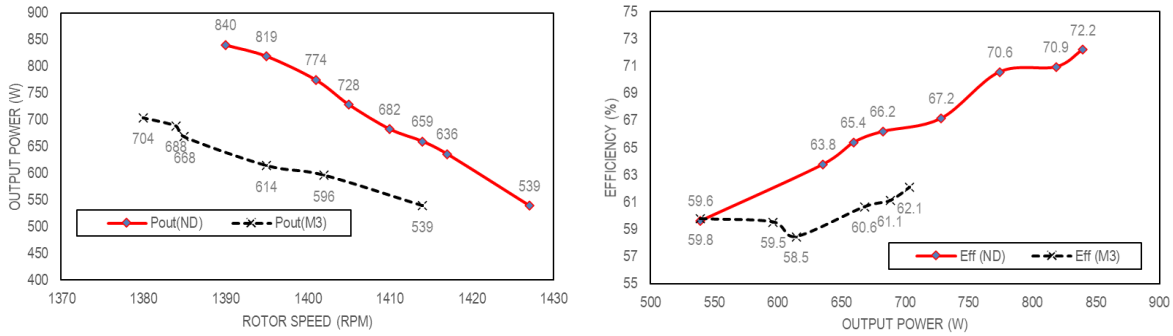

(a) (b)

Figure 8. Characteristics of the correlation between (a) output power and rotor speed and (b) efficiency and motor output power

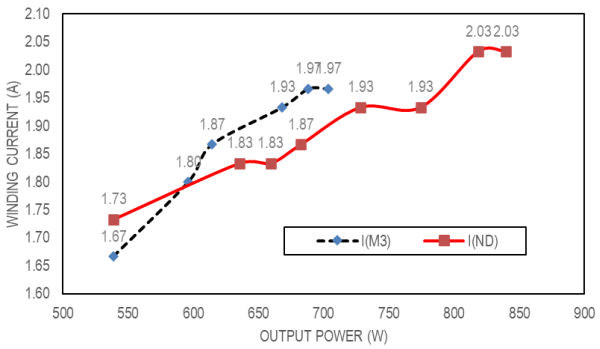

Figure 9. Characteristics of the correlation between winding current and motor output power

Table 1. Particular performance accomplishments of the motors

Object	New design	Traditional design	Enhancement (%)
Quantity of poles	4	4	0
Quantity of windings per slot	110	110	0
Quantity of slots	24	24	0
Load torque (Nm)	5.77	4.87	18.48
Rotor speed (r/min)	1390	1380	0.72
Output power (W)	840	704	19.32
Efficiency (%)	72.2	62.1	16.26
Winding current (A)	2.03	1.97	3.05

(a)

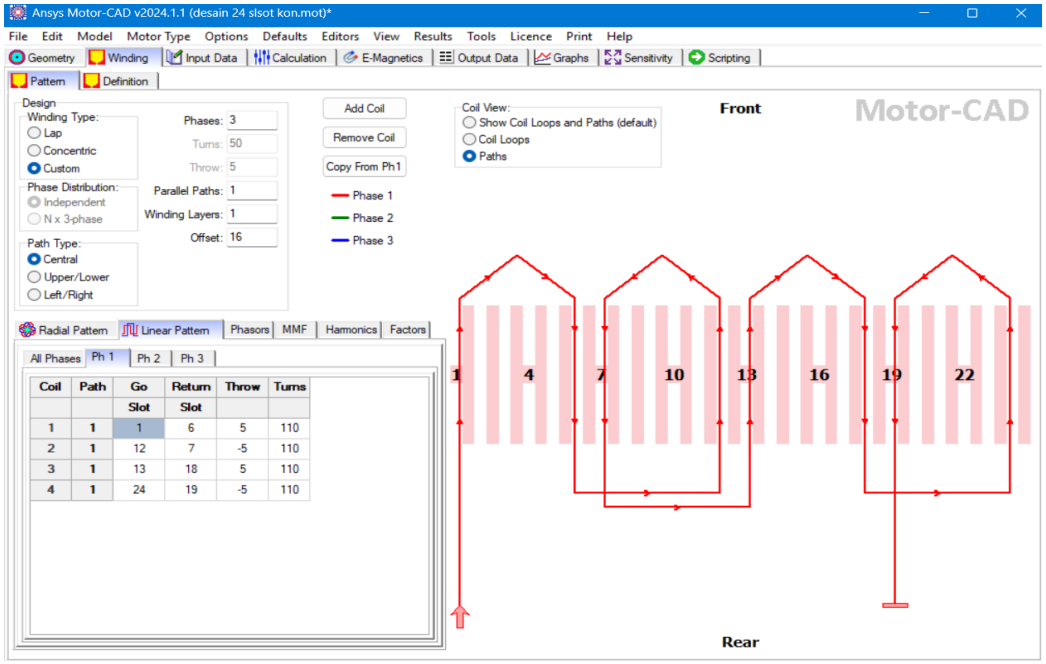

(b)

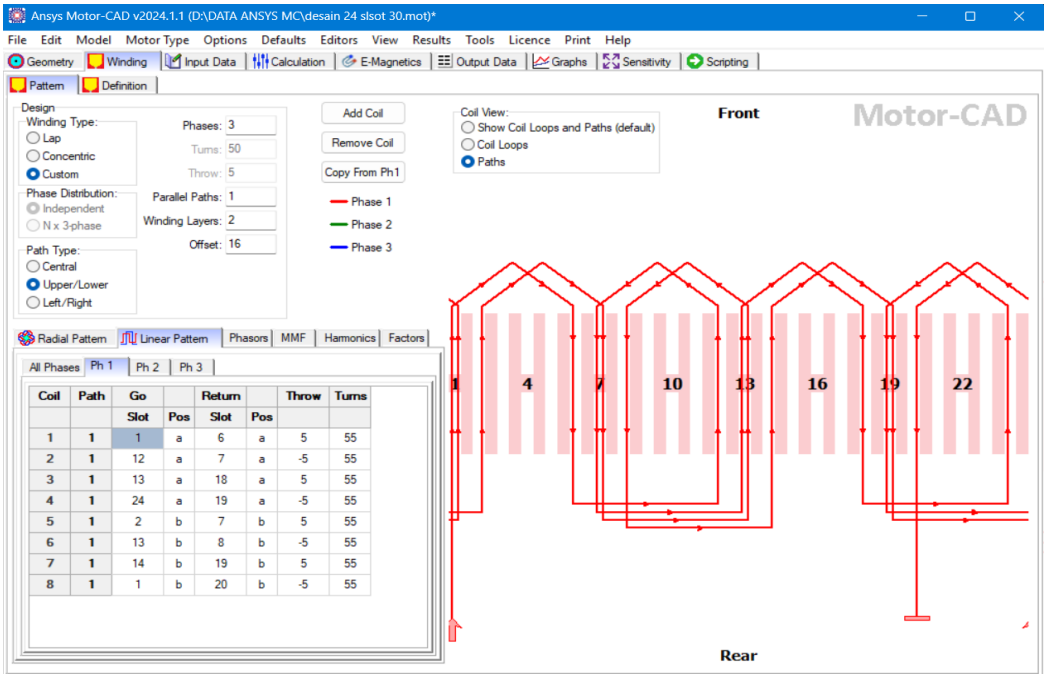

Figure 10. Design form of a 3-phase induction motor coil on phase 1 (phase L1) only using the program 'Ansys Motor-CAD v2024.1.1,' including (a) the coil design on a conventional 3-phase induction motor and (b) the coil design on a new design 3-phase induction motor

(a)

(b)

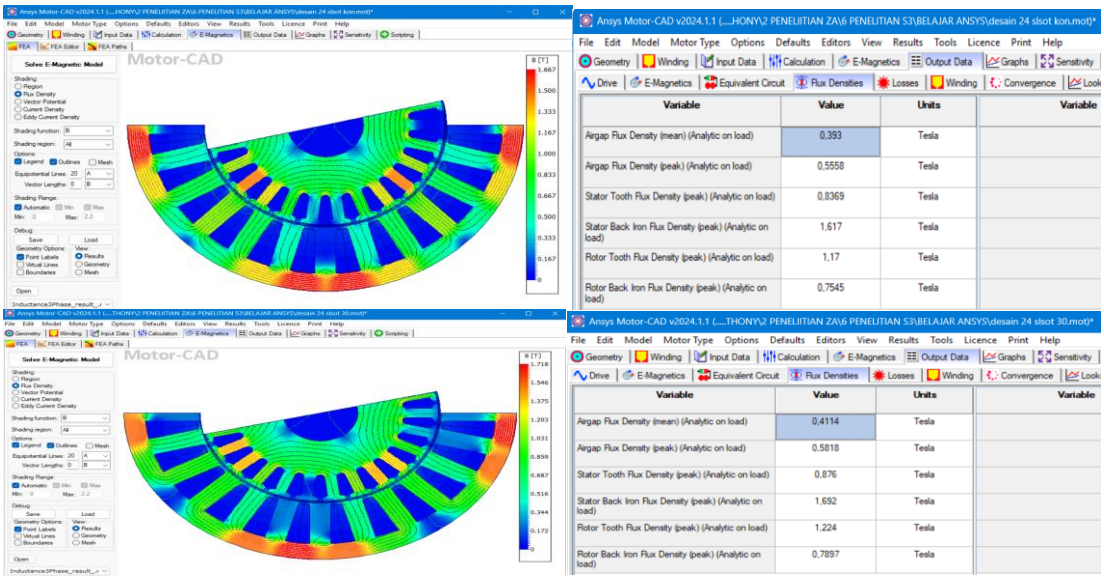

Figure 11. Flux density data for a 3-phase induction motor utilizing finite element analysis (FEA) with the software 'Ansys motor-CAD v2024.1.1' encompasses (a) flux density in a conventional 3-phase induction motor and (b) flux density in an innovative design of a 3-phase induction motor

The architecture of this new motor coil features the formation of unique magnetic poles for each layer, as depicted in Figure 4(c). This arrangement enables the magnetic flux rotation to mimic that of an asymmetrical 6-phase induction motor, resulting in enhanced torque. This situation reduces power losses in the motor coil, thereby improving output power and motor efficiency, as evidenced in (14) and (18). The motor characteristics depicted in Figure 8 and the data presented in Table 1 validate the claim. Figure 8 shows that the new 3-phase induction motor works better than the old one, especially in terms of output power and efficiency, and it is more stable when the load changes. This data is also supported by the simulation results using Ansys Motor-CAD, as shown in Figure 12. Figure 12(a) shows that the output power characteristic waveform of a conventional 3-phase induction motor is below 1400, while Figure 12(b) shows that the output power waveform of the newly designed 3-phase induction motor is higher than 1400. It is clear from these two pieces of information that the new motor design is stronger than the old three-phase induction motor.

Table 1 illustrates that the output power and efficiency of the new design motor are 840 W and 72.2%, respectively. In contrast, the traditional 3-phase induction motor demonstrates an output power and efficiency of 704 W and 62.1%, respectively. The data indicate an increase in output power and efficiency in the new design motor, measuring 19.32% and 16.26%, respectively. This enhancement underscores the efficacy of the new design for optimizing performance, rendering it a more viable choice for applications that demand increased power output and efficiency. These advancements have the potential to result in considerable energy savings and a decrease in operational expenses. Table 2 shows a comparative overview of several ways to improve motor efficiency. By looking at Table 2, which contains several methods to improve motor efficiency, it can be seen that the method in the form of stator winding design development given in this study outperforms other methods.

Figure 9 describes the winding current characteristics of the motor, and it can be seen that, in general, the new design motor operates at approximately the same load but with lower winding current. Although there is a slight increase in the winding current of the new design motor by 3.05% (in Table 1), the overall performance of the new design three-phase induction motor is superior to that of the traditional 3-phase induction motor, with increased output power, motor efficiency, load torque, and rotor speed. By looking at the data in Table 1, it can be seen that this new design motor uses the same stator, rotor, and windings as the conventional motor, except for the shape of the windings. This innovative motor design employs the same materials as traditional 3-phase induction motors; hence, it eliminates the need for costly enhancements to boost motor performance. Therefore, the winding design used in this study is recommended for use in other 3-phase induction motors to improve their performance without significant extra costs. This method improves the motor's overall performance and fosters cost efficiency in production.

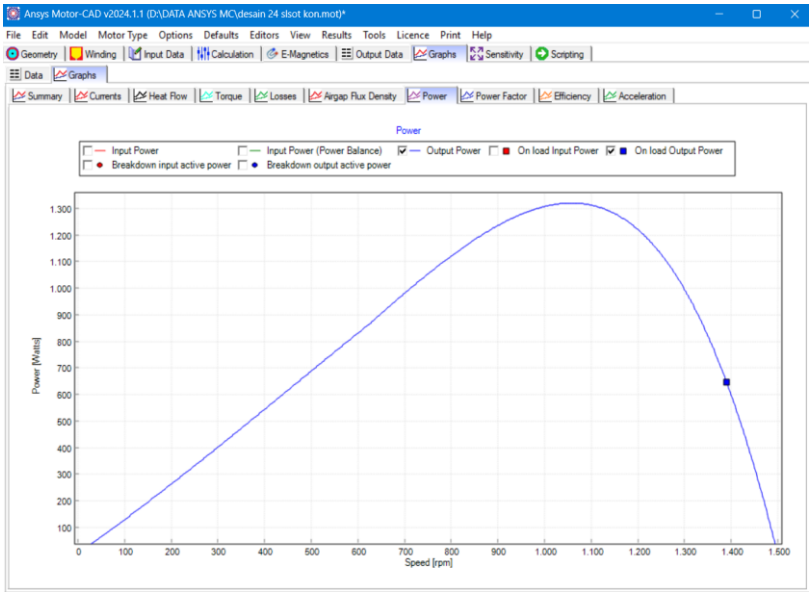

(a)

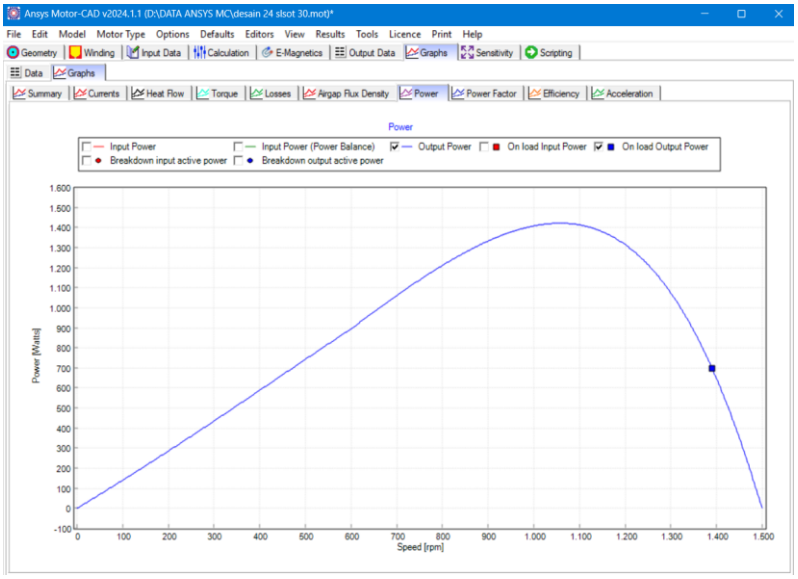

(b)

Figure 12. Characteristic output power vs. speed of a 3-phase induction motor utilizing the 'Ansys Motor-CAD v2024.1.1' application, comprising (a) output power of a standard 3-phase induction motor and (b) output power of an innovative design 3-phase induction motor

Table 2. Comparison of several methods for increasing motor efficiency

Reference	Year	Method	Efficiency enhancement (%)
[5]	2022	Permanent magnet rotor	11.10
[46]	2022	Control system development	7.00
[47]	2023	Rotor slot design	9.25
Our current study	2025	Stator winding design	16.26

5. CONCLUSION

The study found that the new winding design for a three-phase induction motor could enhance its performance by increasing the load torque capacity by 18.48%, the rotor speed by 0.72%, the output power by 19.32%, and the motor efficiency by 16.26%. Although there is a 3.05% rise in the winding current of the motor when it is operating under maximum load conditions, the overall performance of the motor improves as the motor's capability greatly increases. The newly designed three-phase induction motor does not incur any additional expenses because it uses the same materials as conventional three-phase induction motors. We

have full confidence in our solution's ability to enhance the performance of the other three-phase induction motors without imposing astronomical additional costs on the motor. This strategy not only improves the overall reliability of the motors but it also improves their efficiency.

FUNDING INFORMATION

All those who have contributed to making this research a reality have our deepest gratitude. Universitas Andalas, under research contract 104/UN16.19/PT.01.03/PDD/2025, has generously funded this project, and we are quite grateful to them.

AUTHOR CONTRIBUTIONS STATEMENT

This journal uses the Contributor Roles Taxonomy (CRediT) to recognize individual author contributions, reduce authorship disputes, and facilitate collaboration.

Name of Author	C	M	So	Va	Fo	I	R	D	O	E	Vi	Su	P	Fu
Zuriman Anthony	✓	✓	✓	✓	✓	✓	✓	✓	✓	✓	✓		✓	
Refdinal Nazir	✓	✓		✓	✓	✓	✓	✓		✓		✓		✓
Muhammad Imran Hamid		✓		✓	✓	✓	✓	✓		✓		✓		

C : **C**onceptualization
M : **M**ethodology
So : **So**ftware
Va : **Va**lidation
Fo : **Fo**rmal analysis
I : **I**nvestigation
R : **R**esources
D : **D**ata Curation
O : Writing - **O**riginal Draft
E : Writing - Review & **E**diting
Vi : **Vi**sualization
Su : **Su**pervision
P : **P**roject administration
Fu : **Fu**nding acquisition

CONFLICT OF INTEREST STATEMENT

Authors state no conflict of interest.

DATA AVAILABILITY

The authors confirm that the data supporting the findings of this study are available within the article [and/or its supplementary materials].

REFERENCES

[1] S. Zhao, X. Huang, Y. Fang, and H. Zhang, "DC-link-fluctuation-resistant predictive torque control for railway traction permanent magnet synchronous motor in the six-step operation," *IEEE Transactions on Power Electronics*, vol. 35, no. 10, pp. 10982–10993, 2020, doi: 10.1109/TPEL.2020.2975497.

[2] S. Mahfoud, A. Derouich, N. El Ouanjli, N. V. Quynh, and M. A. Mossa, "A new hybrid ant colony optimization based PID of the direct torque control for a doubly fed induction motor," *World Electric Vehicle Journal*, vol. 13, no. 5, 2022, doi: 10.3390/wevj13050078.

[3] W. Pietrowski and K. Górny, "Analysis of torque ripples of an induction motor taking into account a inter-turn short-circuit in a stator winding," *Energies*, vol. 13, no. 14, 2020, doi: 10.3390/en13143626.

[4] Janani Srinivasan, K. Selvaraj, J. Chitrarasu, and R. R, "Induction Motor in short pitch and full pitch winding configurations using FEA," *2016 International Conference on Emerging Technological Trends [ICETT]*, pp. 1–10, 2016.

[5] M. M. TEZCAN and A. S. AKYURT, "Transforming of conventional type squirrel cage induction motor to permanent magnet synchronous motor for improving efficiency on industrial applications," *International Scientific and Vocational Studies Journal*, vol. 6, no. 1, pp. 32–40, 2022, doi: 10.47897/bilmes.1129634.

[6] R. Ni *et al.*, "Efficiency enhancement of general ac drive system by remanufacturing induction motor with interior permanent-magnet rotor," *IEEE Transactions on Industrial Electronics*, vol. 63, no. 2, pp. 808–820, 2016, doi: 10.1109/TIE.2015.2477478.

[7] A. G. Yetgin, M. Turan, B. Cevher, A. İ. Çanakoğlu, and A. Gün, "Squirrel cage induction motor design and the effect of specific magnetic and electrical loading coefficient," *International Journal of Applied Mathematics Electronics and Computers*, vol. 7, no. 1, pp. 1–8, 2019, doi: 10.18100/ijamec.461795.

[8] A. M. Silva, F. J. T. E. Ferreira, M. V. Cistelecan, and C. H. Antunes, "Multiobjective design optimization of generalized multilayer multiphase ac winding," *IEEE Transactions on Energy Conversion*, vol. 34, no. 4, pp. 2158–2167, 2019, doi: 10.1109/TEC.2019.2935009.

[9] Z. Yang, Q. Ding, X. Sun, J. Ji, and Q. Zhao, "Design and analysis of a novel wound rotor for a bearing less induction motor," *International Journal of Electronics*, vol. 106, no. 12, pp. 1829–1844, 2019, doi: 10.1080/00207217.2019.1625971.

[10] A. Glowacz and Z. Glowacz, "Diagnosis of the three-phase induction motor using thermal imaging," *Infrared Physics and Technology*, vol. 81, pp. 7–16, 2017, doi: 10.1016/j.infrared.2016.12.003.

[11] A. Glowacz, "Acoustic based fault diagnosis of three-phase induction motor," *Applied Acoustics*, vol. 137, pp. 82–89, 2018, doi: 10.1016/j.apacoust.2018.03.010.
[12] G. Joksimović, J. I. Melecio, P. M. Tuohy, and S. Djurović, "Towards the optimal 'slot combination' for steady-state torque ripple minimization: an eight-pole cage rotor induction motor case study," *Electrical Engineering*, vol. 102, no. 1, pp. 293–308, 2020, doi: 10.1007/s00202-019-00874-x.
[13] A. Dianov, F. Tinazzi, S. Calligaro, and S. Bolognani, "Review and classification of MTPA control algorithms for synchronous motors," *IEEE Transactions on Power Electronics*, vol. 37, no. 4, pp. 3990–4007, 2022, doi: 10.1109/TPEL.2021.3123062.
[14] Y. Yang, Q. He, C. Fu, S. Liao, and P. Tan, "Efficiency improvement of permanent magnet synchronous motor for electric vehicles," *Energy*, vol. 213, 2020, doi: 10.1016/j.energy.2020.118859.
[15] K. S. Mohammad and A. S. Jaber, "Comparison of electric motors used in electric vehicle propulsion system," *Indonesian Journal of Electrical Engineering and Computer Science*, vol. 27, no. 1, pp. 11–19, 2022, doi: 10.11591/ijeecs.v27.i1.pp11-19.
[16] Z. Anthony, R. Nazir, and M. I. Hamid, "A review of strategies for improving 3-phase induction motor performance," *Andalasian International Journal of Applied Science, Engineering and Technology*, vol. 4, no. 1, pp. 01–12, 2024, doi: 10.25077/aijaset.v4i1.112.
[17] Y.-J. Wang, L. Pierrat, and E. Helerea, "Balancing a three-phase induction motor supplied from a single-phase source with two SVCs," in *2017 International Conference on Optimization of Electrical and Electronic Equipment (OPTIM) & 2017 Intl Aegean Conference on Electrical Machines and Power Electronics (ACEMP)*, May 2017, pp. 268–274. doi: 10.1109/OPTIM.2017.7974982.
[18] V. Malyar, O. Hamola, and V. Maday, "Calculation of capacitors for starting up a three-phase asynchronous motor fed by single-phase power supply," in *2016 17th International Conference Computational Problems of Electrical Engineering (CPEE)*, Sep. 2016, pp. 1–4. doi: 10.1109/CPEE.2016.7738735.
[19] C. Wu, M. Huang, D. Luo, Y. Jiang, and M. Yan, "SiO2 nanoparticles enhanced silicone resin as the matrix for Fe soft magnetic composites with improved magnetic, mechanical, and thermal properties," *Journal of Alloys and Compounds*, vol. 741, pp. 35–43, 2018, doi: 10.1016/j.jallcom.2017.12.322.
[20] M. Aishwarya and R. M. Brisilla, "Design of energy-efficient induction motor using ANSYS software," *Results in Engineering*, vol. 16, p. 100616, Dec. 2022, doi: 10.1016/j.rineng.2022.100616.
[21] P. Sethupathi and N. Senthilnathan, "Comparative analysis of line-start permanent magnet synchronous motor and squirrel cage induction motor under customary power quality indices," *Electrical Engineering*, vol. 102, no. 3, pp. 1339–1349, Sep. 2020, doi: 10.1007/s00202-020-00955-2.
[22] I. Gonzalez-Prieto, M. J. Duran, F. Barrero, M. Bermudez, and H. Guzman, "Impact of postfault flux adaptation on six-phase induction motor drives with parallel converters," *IEEE Transactions on Power Electronics*, vol. 32, no. 1, pp. 515–528, Jan. 2017, doi: 10.1109/TPEL.2016.2533719.
[23] H. S. Che, E. Levi, M. Jones, W.-P. Hew, and N. A. Rahim, "Current control methods for an asymmetrical six-phase induction motor drive," *IEEE Transactions on Power Electronics*, vol. 29, no. 1, pp. 407–417, Jan. 2014, doi: 10.1109/TPEL.2013.2248170.
[24] H. S. Che, M. J. Duran, E. Levi, M. Jones, W.-P. Hew, and N. A. Rahim, "Postfault operation of an asymmetrical six-phase induction machine with single and two isolated neutral points," *IEEE Transactions on Power Electronics*, vol. 29, no. 10, pp. 5406–5416, Oct. 2014, doi: 10.1109/TPEL.2013.2293195.
[25] I. Gonzalez-Prieto, I. Zoric, M. J. Duran, and E. Levi, "Constrained model predictive control in nine-phase induction motor drives," *IEEE Transactions on Energy Conversion*, vol. 34, no. 4, pp. 1881–1889, Dec. 2019, doi: 10.1109/TEC.2019.2929622.
[26] I. S. de Freitas *et al.*, "Twelve-phase induction machine analysis with harmonic injection," in *2018 IEEE Energy Conversion Congress and Exposition (ECCE)*, Sep. 2018, pp. 1611–1618. doi: 10.1109/ECCE.2018.8557360.
[27] M. J. Duran, I. Gonzalez-Prieto, N. Rios-Garcia, and F. Barrero, "A simple, fast, and robust open-phase fault detection technique for six-phase induction motor drives," *IEEE Transactions on Power Electronics*, vol. 33, no. 1, pp. 547–557, Jan. 2018, doi: 10.1109/TPEL.2017.2670924.
[28] M. A. Fnaiech, F. Betin, G. A. Capolino, and F. Fnaiech, "Fuzzy logic and sliding-mode controls applied to six-phase induction machine with open phases," *IEEE Transactions on Industrial Electronics*, vol. 57, no. 1, pp. 354–364, 2010, doi: 10.1109/TIE.2009.2034285.
[29] J. K. Pandit, M. V. Aware, R. V. Nemade, and E. Levi, "Direct torque control scheme for a six-phase induction motor with reduced torque ripple," *IEEE Transactions on Power Electronics*, vol. 32, no. 9, pp. 7118–7129, 2017, doi: 10.1109/TPEL.2016.2624149.
[30] M. J. Duran, I. Gonzalez Prieto, M. Bermudez, F. Barrero, H. Guzman, and M. R. Arahal, "optimal fault-tolerant control of six-phase induction motor drives with parallel converters," *IEEE Transactions on Industrial Electronics*, vol. 63, no. 1, pp. 629–640, Jan. 2016, doi: 10.1109/TIE.2015.2461516.
[31] A. Gautam, O. Ojo, M. Ramezani, and O. Momoh, "Computation of equivalent circuit parameters of nine-phase induction motor in different operating modes," in *2012 IEEE Energy Conversion Congress and Exposition (ECCE)*, Sep. 2012, pp. 142–149. doi: 10.1109/ECCE.2012.6342830.
[32] J. Rao, J. Xu, D. Z. Liu, X. D. Yang, X. P. Cui, and W. M. Ma, "Research of mathematical model of the twelve-phase linear induction motor with double-sided long stators," *Applied Mechanics and Materials*, vol. 416–417, pp. 156–163, Sep. 2013, doi: 10.4028/www.scientific.net/AMM.416-417.156.
[33] A. S. Abdel-Khalik, M. S. Abdel-Majeed, and S. Ahmed, "Effect of winding configuration on six-phase induction machine parameters and performance," *IEEE Access*, vol. 8, pp. 223009–223020, 2020, doi: 10.1109/ACCESS.2020.3044025.
[34] Y. Demir and M. Aydin, "A novel dual three-phase permanent magnet synchronous motor with asymmetric stator winding," *IEEE Transactions on Magnetics*, vol. 52, no. 7, pp. 1–5, Jul. 2016, doi: 10.1109/TMAG.2016.2524027.
[35] Y. Demir and M. Aydin, "A novel asymmetric and unconventional stator winding configuration and placement for a dual three-phase surface PM motor," *IEEE Transactions on Magnetics*, vol. 53, no. 11, 2017, doi: 10.1109/TMAG.2017.2710424.
[36] P. Giangrande, V. Madonna, S. Nuzzo, and M. Galea, "Design of fault-tolerant dual three-phase winding PMSM for helicopter landing gear EMA," *2018 IEEE International Conference on Electrical Systems for Aircraft, Railway, Ship Propulsion and Road Vehicles and International Transportation Electrification Conference, ESARS-ITEC 2018*, 2018, doi: 10.1109/ESARS-ITEC.2018.8607684.
[37] A. S. Abdel-Khalik, A. M. Massoud, and S. Ahmed, "Application of standard three-phase stator frames in prime phase order multiphase machine construction," *IEEE Transactions on Industrial Electronics*, vol. 66, no. 4, pp. 2506–2517, Apr. 2019, doi: 10.1109/TIE.2018.2840497.
[38] J. Laksar, R. Cermak, and K. Hruska, "Challenges in the electromagnetic design of multiphase machines: winding and equivalent circuit parameters," *Energies*, vol. 14, no. 21, p. 7335, Nov. 2021, doi: 10.3390/en14217335.
[39] J. Paredes, B. Prieto, M. Satrustegui, I. Elosegui, and P. Gonzalez, "Improving the performance of a 1-MW induction machine by optimally shifting from a three-phase to a six-phase machine design by rearranging the coil connections," *IEEE Transactions on Industrial Electronics*, vol. 68, no. 2, pp. 1035–1045, Feb. 2021, doi: 10.1109/TIE.2020.2969099.
[40] A. S. Abdel-Khalik, M. S. Abdel-Majeed, and S. Ahmed, "Effect of winding configuration on six-phase induction machine parameters and performance," *IEEE Access*, vol. 8, pp. 223009–223020, 2020, doi: 10.1109/ACCESS.2020.3044025.

[41] I. Gonzalez-Prieto, M. J. Duran, F. Barrero, M. Bermudez, and H. Guzman, "Impact of postfault flux adaptation on six-phase induction motor drives with parallel converters," *IEEE Transactions on Power Electronics*, vol. 32, no. 1, pp. 515–528, 2017, doi: 10.1109/TPEL.2016.2533719.
[42] S. El Daoudi, L. Lazrak, N. El Ouanjli, and M. Ait Lafkih, "Improved DTC-SPWM strategy of induction motor by using five-level POD-PWM inverter and MRASSF estimator," *International Journal of Dynamics and Control*, vol. 9, no. 2, pp. 448–462, 2021, doi: 10.1007/s40435-020-00667-2.
[43] S. Mahfoud, A. Derouich, N. E. L. Ouanjli, M. E. L. Mahfoud, and M. Taoussi, "A new strategy-based PID controller optimized by genetic algorithm for DTC of the doubly fed induction motor," *Systems*, vol. 9, no. 2, 2021, doi: 10.3390/systems9020037.
[44] W. Pei, Q. Zhang, and Y. Li, "Efficiency optimization strategy of permanent magnet synchronous motor for electric vehicles based on energy balance," *Symmetry*, vol. 14, no. 1, 2022, doi: 10.3390/sym14010164.
[45] B. M. Dinh, "Efficiency improvement of squirrel cage induction motor by rotor slot designs," in *Proceedings of the International Conference on Industrial Engineering and Operations Management*, Mar. 2023, pp. 615–623. doi: 10.46254/AN13.20230184.
[46] Z. Anthony and E. Erhaneli, "A new windings design of 24 Slot capacitor-start capacitor-run induction motor," *International Journal of Electrical and Computer Engineering (IJECE)*, vol. 8, no. 5, p. 3463, Oct. 2018, doi: 10.11591/ijece.v8i5.pp3463-3470.
[47] A. Selema, M. N. Ibrahim, and P. Sergeant, "Electrical machines winding technology: latest advancements for transportation electrification," *Machines*, vol. 10, no. 7, pp. 1–29, 2022, doi: 10.3390/machines10070563.
[48] A. M. Silva, F. J. T. E. Ferreira, G. Falcao, and M. Rodrigues, "Novel method to minimize the air-gap MMF spatial harmonic content in three-phase windings," in *2018 XIII International Conference on Electrical Machines (ICEM)*, Sep. 2018, pp. 2504–2510. doi: 10.1109/ICELMACH.2018.8507206.
[49] J. Chen, Y. Fujii, M. W. Johnson, A. Farhan, and E. L. Severson, "Optimal design of the bearing less induction motor," *IEEE Transactions on Industry Applications*, vol. 57, no. 2, pp. 1375–1388, 2021, doi: 10.1109/TIA.2020.3044970.
[50] S. I. Suriano-Sánchez, M. Ponce-Silva, V. H. Olivares-Peregrino, and S. E. De León-Aldaco, "A review of torque ripple reduction design methods for radial flux PM motors," *Eng*, vol. 3, no. 4, pp. 646–661, 2022, doi: 10.3390/eng3040044.
[51] S. M. S. H. Rafin, Q. Ali, S. Khan, and T. A. Lipo, "A novel two-layer winding topology for sub-harmonic synchronous machines," *Electrical engineering*, vol. 104, no. 5, pp. 3027–3035, 2022, doi: 10.1007/s00202-022-01531-6.
[52] J. F. Gieras, *Electrical machines*. Boca Raton: CRC Press, 2017.: CRC Press, 2016. doi: 10.1201/9781315371429.
[53] S. J. Chapman, *Electric machinery fundamentals - 5th edition*, 5th ed. McGraw Hill, 2011.

BIOGRAPHIES OF AUTHORS

Zuriman Anthony is a lecturer in the Department of Electrical Engineering at the Institute of Technology Padang (ITP), Padang, Indonesia. He received his B.E. in electrical engineering from Padang Institute of Technology, Padang, Indonesia, in 1996. He received the M.Eng. degree in electrical engineering from Gadjah Mada University, Yogyakarta, Indonesia, in 2002. He has always been active in various research activities, especially in the fields of electrical machines and electrical power systems. He is currently completing a doctoral program in the electrical engineering department at Universitas Andalas, Padang, Indonesia. His areas of interest are energy conversion, electrical machines, and electrical power system analysis. He can be contacted at email: zuriman@itp.ac.id.

Refdinal Nazir is a lecturer in the Electrical Engineering Department at the Universitas Andalas, Indonesia. Refdinal Nazir received his B.E. and M.Tech. degrees in Electrical Engineering from the Bandung Institute of Technology (ITB) in Bandung, Indonesia, in 1985 and 1986, respectively. He received a Ph.D. degree from the University of Technology Malaysia (UTM), Johor Bahru, Malaysia, in 1999. He has some experience in solving energy modelling and planning problems using LEAP, HOMER, and RETScreen software. He has published several papers at various national and international conferences and has done a number of in-house and industry projects. His areas of interest are electric machines, electric power and energy, renewable energy sources, microgrids, energy conservation, and energy efficiency. He can be contacted at email: refdinalnazir@eng.unand.ac.id.

Muhammad Imran Hamid is a lecturer in the Electrical Engineering Department at Universitas Andalas in Indonesia. Muhammad Imran Hamid received his B.E. in electrical engineering from Hasanuddin University in 1996. He received the M.Eng. degree in Electrical Engineering from the Bandung Institute of Technology in 2001. He received a Ph.D. degree from the Universiti Teknologi Malaysia in 2014. His areas of interest are renewable energy, power electronics, and power quality. He can be contacted at email: imran@eng.unand.ac.id.